Original Article

The Arabidopsis trichome is an active mechanosensory switch

Li Hong Zhou[1,2,3], Shao Bao Liu[1,2,3], Peng Fei Wang[2,4], Tian Jian Lu[2], Feng Xu[2,5], Guy M. Genin[1,2†] & Barbara G. Pickard[1,3†]

[1]*Department of Mechanical Engineering & Materials Science,* [2]*Bioinspired Engineering & Biomechanics Center,* [3]*Gladys Levis Allen Laboratory of Plant Sensory Physiology, Biology Department, Washington University in St. Louis, St. Louis, MO, 63130, USA,* [4]*Qian Xuesen Laboratory of Space Technology, China Academy of Space Technology, Beijing, 100094, China and* [5]*Ministry of Education Key Laboratory of Biomedical Information Engineering, School of Life Science & Technology, Xi'an Jiaotong University, Xi'an, 710049, China*

ABSTRACT

Trichomes ('hair cells') on *Arabidopsis thaliana* stem and leaf surfaces provide a range of benefits arising from their shape and disposition. These include tempting herbivores to sample constitutive toxins before they reach the bulk of the tissue. We asked whether, in addition, small mechanical disturbances such as an insect can make elicit signals that might help the plant respond to herbivory. We imaged, pressed and brushed trichomes in several ways, most notably with confocal microscopy of trichomes transgenically provided with apoplastic pH reporter apo-pHusion and cytosolic Ca^{2+} reporter cameleon. In parallel, we modelled trichome wall mechanics with finite element analysis. The stimulated trichome focuses force on a pliant zone and the adjoining podium of the stalk. A buckling instability can further focus force on a skirt of cells surrounding the podium, eliciting oscillations of cytosolic Ca^{2+} and shifts in apoplastic pH. These observations represent active physiological response. Modelling establishes that the effectiveness of force focusing and buckling is due to the peculiar tapering wall structure of the trichome. Hypothetically, these active mechanosensing functions enhance toxin synthesis above constitutive levels, probably via a priming process, thus minimizing the costly accumulation of toxins in the absence of herbivore attack but assuring rapid build-up when needed.

Key-words: apoplast pH shift; calcium oscillation; force focusing; mechanical buckling; mechanosensing; wall taper.

INTRODUCTION

Arabidopsis trichomes have been studied extensively to understand their development, differentiation and physiology, and they have been shown to have many passive functions that benefit the leaves that produce them. These passive benefits include obstructing airflow to create a microshell of relatively high humidity, reflecting bright light to protect against photodamage and overheating (Suo *et al.* 2013), forming a mechanical barrier against insect attack and forming a gantlet of tempting, easy-to-bite toxin-rich structures, which, if tasted by

an insect, might hasten its departure before it broke the integrity of the pavement cell layer protecting the photosynthetic cells and vascular tissue (Dai *et al.* 2010; Frerigmann *et al.* 2012). The rupture of glandular trichomes on tomato (*Solanum lycopersicum*) plants has been shown to trigger defensive responses (Peiffer *et al.* 2009).

However, it is surprising that Arabidopsis trichomes have not yet received careful attention from the perspective of active structures, as systems that can enable repeated transduction of mechanical responses without rupturing. The observation of force-focusing properties of the trichome leads us to propose that they serve as mechanosensors that trigger active plant responses when stimulated, even in the absence of a rupture. We have found mechanoresponses within the papillate branched stalk wall system as well as in the walls where the trichome and surrounding skirt cells make contact and in the skirt cells and the adjacent epidermis. The complexities of these aspects of mechanosensing and response make it practical to consider them separately. The present paper addresses the latter.

A motivation for pursuing this line of research has been the knowledge that, whereas Arabidopsis leaves manufacture toxins that deter microbial infection and herbivory by insects and other animals, the manufacture and the storage of the toxins have costs to the plant (Paul-Victor *et al.* 2010; Züst *et al.* 2011). Therefore, plants maintain limited constitutive levels of active defence compounds but synthesize extra compounds when the receptor systems are alerted by various stressors. Given the apparent costs and benefits as well as possible varieties and specificities of responses, it would seem useful for Arabidopsis to have an early warning system such that when insects alight on a leaf or crawl over it, the mechanical disturbance could be utilized as a trigger to prime or up-regulate pathways of toxin synthesis and perhaps release. The structure of the trichome system seems well suited from a mechanical standpoint to be a candidate for this. Part of the motivation for testing our hypothesis that trichomes serve as specialized mechanosensors was to form a foundation for future studies that evaluate whether such mechanosensing contributes to interactions between plants and insects.

In the initial test of the biophysical aspects of our hypothesis, we present evidence that mechanical perturbation of the distal part of the trichome gives rise to large Ca^{2+} oscillations within the proximal skirt cells that surround the expanded podial region of the trichome stalk. We demonstrate that this response

is mediated by mechanical switching based on a structural buckling instability at the podium and the adjacent pliant zone of the stalk. While moderate mechanical stimulation elicits the Ca^{2+} oscillations, stronger stimulation further results in alkalization of the apoplast in the walls of the skirt cells and the surrounding pavement cells.

MATERIALS AND METHODS

Plants

To permit assessment of anticipated mechanically elicited pH and Ca^{2+} changes, we utilized three plants with transgenic bioreporters. Seeds of *Arabidopsis thaliana* var. Columbia transformed with apoplastic apo-pHusion or with cytoplasmic pHusion were a gift from Gjetting, Schulz, and Fuglsang (Gjetting *et al.* 2012), creators of these lines. As extensively detailed by these authors, these lines can provide valuable dynamic information about relative pH, but using these lines can be problematic for determining absolute pH values. Seeds with transgenic cameleon Y3.6 were a gift from the Simon Gilroy and Gary Stacey laboratories (Monshausen *et al.* 2008; Tanaka *et al.* 2010). This line enables tracking of cytosolic Ca^{2+} by using confocal fluorescence microscopy, as described in the next section. Seeds were planted in Fafard superfine germination mix from SunGro Horticultural Products (Agawam, MA, USA), held in a cold room for 2 d and grown in a 22 °C chamber with some air movement and cycling with 16 h of 0.1 $W\,m^{-2}$ (or 150 $\mu mol\,m^{-2}\,s^{-1}$) white fluorescent light and 8 h darkness. Plants containing the viral movement protein MP17 fused to green fluorescent protein, known to localize to plasmodesmata (Link *et al.* 2011), were imaged by David W. Ehrhardt, who has gifted Supporting Information Movie S1 to our project.

Mounting and stimulating for microscopy

Rosette leaves more than 5 mm and less than 10 mm long, that had finished at least most of their growth, were excised from plants 10 days old and mounted in water with the trichomes of interest facing the bottom glass slip or extending free off the side of the leaf. Two methods of stimulation were used. Persistent overall flexure of mounted trichomes was accomplished by gently pressing downwards against the silicone-grease-supported upper glass slip. Flexure before mounting was achieved by pressing a region of stalk or branch with the tip of a moistened Sceptre Gold II model 202 sable hair paintbrush (Winsor & Newton, http://www.winsornewton.com). Because the leaves were curved and wavy rather than flat, the trichomes were checked carefully to determine which were well positioned for controlled stimulation and imaging. Any minor stimulation due to handling must have contributed to control as well as experimental images and was not noticeable.

Microscopy

Several different microscopes were used, depending on the purpose and their availability. For confocal microscopy, a Leica SP8 microscope (Leica Microsystems, http://www.leica-microsystems.com), with white light (470–670 nm) laser and a resonant scanner, was used for most images, but a Nikon A-1 (Nikon Instruments, http://www.nikoninstruments.com) was used to obtain Fig. 1b–d; 20 X oil immersion objective lenses were used. For apo-pHusion, excitation was carried out at 488 nm, and capture was carried out at 500–550 nm for the enhanced green fluorescent protein (EGFP) component; for the red fluorescent component mRFP1, the respective values were 558 and 580–610 nm. For cameleon, excitation was carried out at 458 nm, and emission was captured at 473–505 and 526–536 nm (Monshausen *et al.* 2008; Swanson & Gilroy 2013). Image stacks with cubic voxels were examined in several ways both with the microscope software and with Fiji (Schindelin *et al.* 2012). Figures were prepared by brightest voxel projections of stacks. As is standard, confocal fluorescence microscopy data were recorded as spatial arrays of fluorescence emission intensity that can be represented as greyscale-type images of arbitrarily chosen colour. For pHusion images, different colours were assigned for each of the two channels of confocal fluorescence microscopy data, and, again, by following the standard protocol, composite images were generated by superposing these data. Red and green fluorescence are represented by red and green pseudocolours, respectively, with yellow indicating overlap. For cameleon images, the ratio of the Förster resonance energy transfer (FRET) channel to the excitation channel is represented by a rainbow scale, following the standard protocol for this reporter.

Although some varieties of Arabidopsis have regions of autofluorescence, with our wild-type plants only extremely weak autofluorescence was detected by coupled sweeping of the excitation and emission spectra used for the bioreporters. For experiments with trichomes of plants grown in different environments, these controls must always be run because autofluorescence can depend on growth conditions. Additionally, because one dominant source of leaf autofluorescence is chlorophyll, the bioreporters are designed to avoid excitation in the chlorophyll's absorption bands, especially at 420–460 nm, and to minimize collection in chlorophyll's emission bands above 600 nm (cf. Hepler & Gunning 1998).

Figure 1a versus Fig. 1b–d appear pseudocoloured slightly differently because of the different confocal captures and the associated microscope software. Moreover, with the Nikon image stacks, which required relatively long exposures per plane, the top of the stack was saturated and the mRFP1 contributed disproportionately to the image — that is, the green hue was somewhat yellowed. However, a second reason for the slight yellowing is a real pH change. The complexity of the wall response is very important but is greater than what can be considered in the present gross microscopy analysis.

Differential interference contrast (DIC) images of wild-type trichomes were captured with the Leica SP8 microscope. Ultraviolet (UV) transmission images of wild-type trichomes (Fig. 5a) were captured with a Zeiss fluorescence microscope (Carl Zeiss, Oberkochen, Germany) with non-fluorescing white paper placed to diffuse the incident light. Imaged

trichomes were protruding freely from the leaf margin, assuring that UV light was transmitted only through the trichome and not through other cells.

Mechanical model

A three-dimensional computational mechanical model of a trichome was studied to test the hypothesis that the tapered shape of the trichome promoted force focusing and buckling. The model began with a three-dimensional representation of a trichome generated based on microscope images by using standard computer-aided design software (Creo, PTC, Needham, MA, USA). An STL (stereolithography) format file was exported from this software and imported into a standard finite commercial finite element analysis software package (ABAQUS, Dassault Systèmes, Vélizy-Villacoublay, France).

By using the finite-element package, the cell wall of the trichome was represented as an elastic, isotropic shell. This shell was discretized into smaller elements that represent Mindlin–Reissner plates (ABAQUS S4 shell elements). In the baseline studies of an idealized trichome, the thickness of these plates was varied spatially within the trichome stalk by averaging the wall thickness at each height and generating an axisymmetric idealization. In this idealized trichome, the wall thickness varied from ~6 μm in the stalk wall to ~1.5 μm in the pliant zone wall. Two fictional trichomes were also generated for comparison studies. For these, the thickness of the cell wall throughout the trichome was fixed at either the minimum (1.5 μm) or the maximum (6 μm) cell wall thickness that was present in the idealized trichome. In all cases (idealized and fictional trichomes), the skirt cells surrounding the trichome base were modelled through a boundary condition in which both displacement and rotation were fixed to zero at the base of the trichome.

The number of elements used in the studies was chosen by following standard procedures to ensure that the finite element estimates were accurate. These involved careful mesh convergence studies, in which elements were reduced in size until the energy absorbed by the model after buckling of the trichome changed less than 1% with addition of additional elements. In all cases, convergence was reached with an average element size of ~2 μm. A representative finite element mesh is presented in the Supporting Information Fig. S1.

The model was used to study the focusing of force to the base through a buckling instability. Various interactions with insects were modelled by applying displacements at each of three different points; in each case, two values of displacement were studied. For the case of a trichome with wall thickness that was varied spatially, elastic buckling occurred and the mechanical response was obtained by applying these displacements in increments sufficiently small to ensure numerical convergence. Simulations were performed on a workstation equipped with dual-quad core Intel Xeon processors and 24 GB of random-access memory (HP Z800, Hewlett-Packard, Palo Alto, CA, USA).

RESULTS

Trichome apoplasts have two pH compartments, one unusually alkaline

The initial experiments performed to characterize the unstimulated Arabidopsis trichome expressing the pH bioreporter apo-pHusion proved interesting in themselves. The most striking result is that the apoplast of the wall is dramatically more alkaline than either the apoplasts of the immediately surrounding cells or the epidermal cells in general (Fig. 1a). In order to compare the fluorescent emissions by the trichome with those by the surrounding cells, it is essential to understand the structure of the fluorochrome reporter, developed and extensively described by Gjetting *et al.* (2012). The fluorochrome reporter is composed of tandem-linked EGFP and mRFP1 and thus references green fluorescence varying over a relatively basic range to independent red fluorescence that is comparatively invariant over a relatively acidic range; its pKa is about 6. Its response is generally too complex and non-linear to invite pH quantitation in the present case, but it is superb for assessing apoplastic pH differences and shifts.

Apo-pHusion identified a number of trichome features that have not been well visualized previously. As noted earlier (and see all parts of Fig. 1), the overall pH of the branches and the upper region of the stalk is relatively alkaline. There is usually a little more mRFP1 fluorescence in the branches than in the stalk; this represents a complicated situation in that cross-sectional views of branches, such as those in Fig. 1b, can reveal a relatively acidic contribution from an internal wall layer. Compartmentalization within these walls is complex and is the focus of an ongoing study. The EGFP fluorescence falls off somewhat where the branches join the stalk and falls off conspicuously in a ring near the base that we term the 'pliant zone'. Possibly the apoplast is not readily accessible to the bioreporter in the pliant zone, but conceivably the pH is graded to a more acidic range a little too low for much EGFP fluorescence, while local molecular aggregations inhibit fluorescence of mRFP1. These possible reasons for the failure to fluoresce are discussed by the originators of the reporter (Gjetting *et al.* 2012). As confirmed by standard staining protocols and transmission electron microscopy (TEM), papillae, which appear in our images as scattered fluorescent ovals, are present on much of the aerial trichome but are much reduced in size and surface density in the pliant zone. The appropriateness of the term 'pliant zone' was confirmed when, for a related project, trichomes were fixed for regular staining procedures or fast-frozen for TEM: the trichome structure crumpled in this region (not shown).

Basal to the pliant zone, the trichome stalk expands into a podium that fluoresces predominantly but not exclusively green (colour ratio dominated by green), where it rises out of the surrounding cells. The proximal fluorescence boundary is distinct, and the subsurface part of podium is non-fluorescent; hence, the bioreporter data suggest that the subsurface podium wall has a special character.

The non-fluorescent subsurface podium is surrounded by a skirt of cells that, in controls and even in mildly stimulated trichomes, have distinctly acidic walls. Although skirt morphology was a somewhat variable feature of the trichome system,
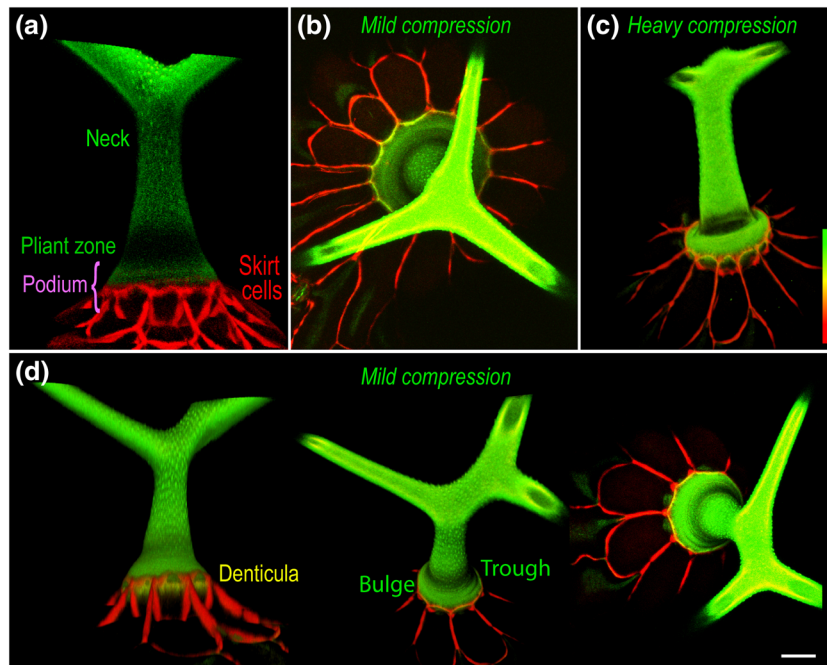
Figure 1. Gross confocal views of mature trichomes. Bioreporter apo-pHusion fluorescence indicates relative pH, spatially differentiating wall composition. (a) Unstimulated trichome system, with some mechanically critical features identified. The subsurface podium, surrounded by skirt cells, does not fluoresce and the pliant zone fluoresces minimally. (b) Viewing a moderately compressed trichome from above shows mechanoresponse from a different perspective. Branches usually display yellower overall in the results of mechanical stimulation. However, where the branches are optically cut the inner and outer portions of the wall are seen to grade in pH from more acidic to more basic. (c) A heavily compressed, hence forward-leaning, trichome viewed from the side shows more extreme features of buckling and bulging, with a trough clearly evident inside the bulge. See more details in Supporting Information Movie S2. (d) Three views of one trichome compressed moderately from above help visualize details of buckling, with good views of trough and bulge formation and also of denticula with shifted pH. Scale: relative pH from higher (green) to lower (red); the pKa for the bioreporter is about 6. Bar: 20 μm.

the position of the trichome on the leaf determined much of this variation: for example near the elongate epidermal cells near the vascular tissue, the skirt tends to be very asymmetric or not well differentiated from the general epidermis. Skirts can have few cells or many cells, can rise high around the podium or lie flat, can be very geometric or rather irregular and can be composed of one or more cell rings. Therefore, we systematically experimented with the trichomes that were situated halfway along the leaf axis but near the leaf margin, for they usually have relatively simple, only slightly asymmetric skirts.

The contribution of the branches to the antennal structure, of critical mechanical interest, is often of simple pattern as viewed from above in Fig. 1b. But like the skirt cells, the branches are variably arranged (compare Fig. 1d). Regardless, they are spread out sufficiently for alighting or crawling insects to make contact with them.

The trichome is prone to force focusing and reversible buckling

To discover the morphological effects of mechanical stimulation, we compressed the trichomes of transgenic leaves mounted between two glass coverslips; the results are exemplified in Fig. 1. This necessarily displaced the branches somewhat, but moderate compression did not markedly bend the stalk or cause it to lean noticeably. Rather, the pliant zone bulged and wrinkled slightly

(compare Fig. 1d, which shows three views of such a trichome, with the control in Fig. 1a). However, stronger compression led to a buckling instability localized in the pliant zone and resulting in a conspicuous trough with a surrounding bulge (Fig. 1c and Supporting Information Movie S2 of the image stack from which it was projected). Even with the strong, slightly asymmetric, compression shown in Fig. 1c, the stalk axis remained straight, bending at the pliant zone. With yet stronger compression, even with highly asymmetrical compression, most of the stalk stayed fairly straight but bent at the pliant zone. Thus, the remotely applied force was focused to the base of the trichome.

Buckling was reversible and therefore not likely due to damage. This was seen in two ways: firstly, by observing a return after releasing the axially applied compressive force and, secondly, by observing a return after the trichomes were laterally stimulated by brushing with a soft paintbrush. Deliberately inflicted trichome damage in another extensive research project was seen to result not only in irregular and irreversible bending but also in drastic shifts in Ca^{2+} and H^+ distribution in the trichome branches and stalk.

Ca^{2+} oscillation in skirt cells: buckling creates physiological signal

Because the transfer of force to skirt cells from the podium is one of the most dramatic effects of mechanically stimulating

the branches and stalk and because Ca^{2+} is a ubiquitous signalling ion in both plants and animals and often mediates responses to mechanical stimulation (Allen *et al.* 1999; Clapham 2007; Monshausen & Haswell 2013), it was of interest to learn whether the cytosolic Ca^{2+} of skirt cells responds when force is focused on them via the podium. In particular, regulatory information is often conveyed by triggered oscillation (Monshausen *et al.* 2008; Tanaka *et al.* 2010), so sequential imaging was carried out.
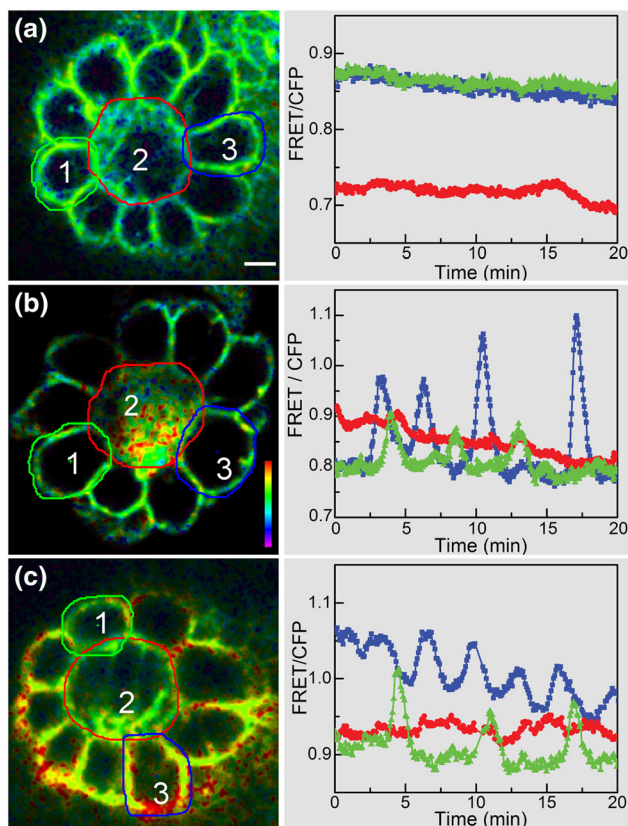
Figure 2. Ca^{2+} oscillations elicited in skirt cells. Cytosolic Ca^{2+} was indexed by yellow cameleon fluorescence, showing that mechanoelectrical energy has been translated to chemical energy in the form of a physiological signal. Movies transecting skirt cells (Supporting Information Movies S3 and S4) are represented at left by single image planes in which regions of analysis are marked and at right by plots of FRET over cyan fluorescent protein fluorescence. (a) Control, showing no oscillatory responses. Trichome with stalk asymmetrically brushed (b) and stimulated (c) as in Fig. 1c: oscillatory responses occur in the skirt cells but not in the trichome podium. Traced selections in the left panels identify the region over which fluorescence was averaged to obtain the time courses of matching colour in the right panels. Red traces represent the podium of the trichome, in which Ca^{2+} did not oscillate. Numbers within traces correspond to numbers in Supporting Information Figs. S3 and S4, where oscillations are graphed for all the skirt cells of Fig. 2b,c and statistics are provided. It should be noted that it is impossible to outline a cell perfectly at this resolution; ROIs as drawn contain contributions from adjacent cells, and in particular this must make the podia of Fig. 2b,c appear more irregular than they are. The colour scale for images indicates the range of cytoplasmic Ca^{2+} concentration with red for high and violet for low. Size bar = 20 μm.

Cytosolic Ca^{2+} in the skirt cells of plants expressing cytoplasmically targeted Ca^{2+} bioreporter yellow cameleon YC3.6 (Tanaka *et al.* 2010; Swanson & Gilroy 2013) indeed underwent oscillation. Figure 2 shows the results of monitoring the fluorescence in cytoplasmic regions of interest (ROIs), circled in each of the images for corresponding display in the plots of FRET/cyan fluorescent protein fluorescence. Whereas unstimulated controls (Fig. 2a) presented only a slow drift of the signal for the selected ROIs, cytoplasmic Ca^{2+} in the skirt cells oscillated unequivocally in response to mechanostimulation by compression of the trichome between glass slips (compare Fig. 2b with Fig. 1) or by brushing the trichome at the junction by using a sable paintbrush (Fig. 2c). In order to simplify presentation, Fig. 2 shows only selected oscillations, but each skirt cell was analysed for each experiment. For example, Supporting Information Movies S3 and S4 show the cameleon shifts in images of all skirt cells of Fig. 2b and 2c. Supporting Information Figs 3 and 4 display oscillation analyses for each cell in these two movies as well as statistical validation. Oscillations were asymmetrically distributed in pressed trichome systems; perhaps they were most dramatic in cells on the buckled, rather than stretched, side of the podium, but the depth of focus in these experiments precludes directional information. The independence of the skirt cell oscillations in the compressed and stretched sides (compare the ROIs) suggests that they were the direct result of tension from the buckled podium experienced individually by each cell. It could be argued that oscillations were somewhat more symmetrically distributed in the brushed trichomes, for which the stimulus vector could sweep over an arc; but quantitation would be challenging.

The individual actions of the cells suggests that, despite the abundance of plasmodesmata connecting the individual skirt cells with each other and with the podium (Supporting Information Movie S1), they must have been
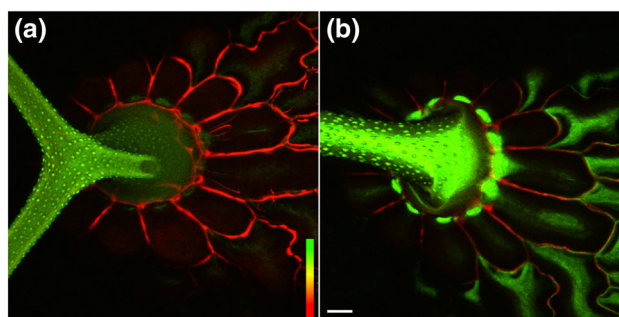

Figure 3. pH responses in skirt cell walls. (a) Trichome before mechanical stimulation; the walls of skirt cells are relatively acidic. (b) Trichome bending at pliant zone, resulting in leaning far towards the epidermis; the walls of skirt and surrounding epidermis have become more basic. The pH in walls at the region of contact between podium and skirt cells has become so high that the difference between them cannot be distinguished. (Denticula, newly discovered features at the contact zone, do not show in the controls but show in mildly stimulated trichomes in Fig. 1. Some denticular proteins are identified but are best discussed elsewhere.) Scale: relative pH from higher (green) to lower (red). Bar = 20 μm.
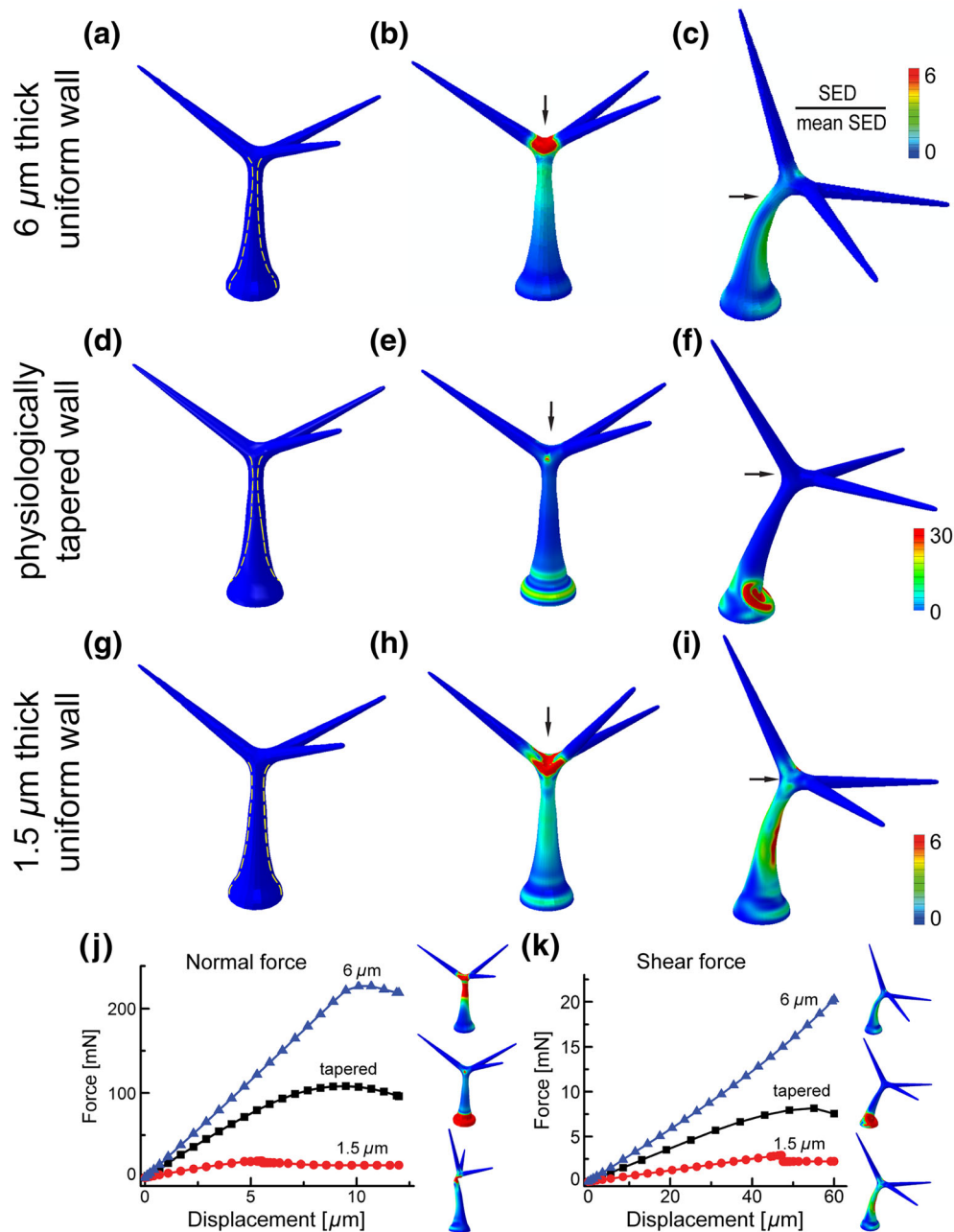
Figure 4. Trichome wall morphology enhances a podium buckling instability. The tapered wall (d–f) of a three-dimensional digitally constructed trichome focuses force on the podium and thus to the skirt region (compare Fig. 2) at which Ca^{2+} oscillations were observed. Strain energy density (colour bars) has been normalized by mean strain energy density in the loaded trichome; contours represent elevation or reduction relative to the mean. Three wall geometries were compared: 1.5 μm uniform walls (g–k), physiologically tapered walls (1.5–6 μm thick, d–f,j,k) and 6 μm uniform walls (a–c,j,k). Only the physiologically tapered trichomes focused force on the podium (e,f) and buckled at the podium (j,k) as in the experiments. Note that Fig. 4e,f expands the scale used for Figs. 4b,c and 4h,i in order to reveal more details of strain energy distribution. The fivefold greater range emphasizes the immense focusing of strain energy to the podium by physiologically tapered trichomes. The small images in Fig. 4j,k are scaled from 0 to 6 and illustrate systematically greater stress application than in the large images above them.

essentially closed while experiencing force during our experiments. It is documented that cytosolic Ca^{2+} can close plasmodesmata transiently (Holdaway-Clarke *et al.* 2000). It is likely that the primary function of these connections is to provide water and substrate from the neighbouring cells and in turn the phloem for trichome development

and for the synthesis of materials for transport into the papillae.

The occurrence of Ca^{2+} oscillations in the skirt cells of the trichome when force was applied to the branches or junction by compression (Fig. 2b) or by brushing (Fig. 2c) strengthens the argument that the trichome is indeed a mechanosensory system

specifically evolved to transmit and focus force on specialized responder cells.

Skirt cell wall pH shift: another physiological effect of buckling

A further demonstration of the physiological impact of trichome buckling was prominent when trichomes were strongly pressed, so that they tended to lean towards the epidermis as shown in an extreme case in Fig. 3. The apoplastic pH in the walls of the skirt cells and also the surrounding epidermis underwent a conspicuous shift towards alkalinity. In interpreting the dramatically decreasing intensities of the red pixels in the periclinal skirt and epidermal cell walls in Fig. 3, recall that apo-pHusion registers pH with relative brightness but little response to wavelength within its responsive range, with green emission emerging in a strongly wavelength-dependent manner in the higher pH range. Further, strain cannot be uniform across the surficial periclinal walls. Realize also that the strain in the anticlinal walls should be less than that in the surficial periclinal walls and that images of anticlinal walls contain contributions from deeper-lying planes. Having taken the subtleties of apo-pHusion response into account, there seems to be an even bigger response in the pavement cells than in the skirt cells. This implies that bending a single trichome can have a far-reaching effect.

Because the pH differences between the unstimulated or mildly stimulated papillate trichome and skirt cell walls are so extreme, it might be postulated that apo-pHusion is not working properly and is more influenced by wall chemistry than by pH. However, the colour shifts in Fig. 3 negate this possibility for the skirt cells. Further, in a long series of experiments with another purpose, we checked for function and found that trichome wall apoplasts yellow and redden in a complex pattern with strong stimulation. Evidently the apoplastic reporter is functional in both cell types.

Wall taper facilitates buckling at the podium

In all compressions of all real trichomes studied, buckling was localized to the region we term the pliant zone where the stalk widens into the podium (Fig. 1). This was expected in part from the broadening of the structure, as in buckling of baby bottle nipples (Supporting Information Fig. S2). We therefore studied whether structural (as contrasted with material) features of the trichome could promote force focusing and buckling by using computer simulations of the response of representative fictional trichomes (Fig. 4). The subsurface wall of the podium was treated as the base to which the projecting portion was attached.

The mechanical response of a structure such as a trichome involves bending or flexural deflection at lower levels of loading. Demonstrating this, we first studied a fictional trichome with a uniform cell wall thickness of $1.5\,\mu m$ (Fig. 4g). In response to both axial and lateral forces that might be associated with herbivory, the work of loading the trichome was stored as strain energy. However, this storage of energy was non-uniform due to structural factors that concentrate force (stress) locally. When this trichome was compressed axially (Fig. 4h), some force focusing was evident at the podium (light blue band of mildly elevated strain energy density), but the greatest density of strain energy was found at the top of the stalk, just beneath the branches (red region).

At sufficiently high levels of loading, all structures undergo collapse through material failure, a buckling instability or both. As an example, the same thin-walled fictional trichome when loaded with a lateral compressive force component first responded stably in flexure, much like the way it responded to axial loading (Fig. 4i). However, beyond a critical force, it buckled about halfway along the stalk's length. The effects of different loading strengths are graphed in Fig. 4j, where some small figures exemplifying relatively high loading are shown as well. The analyses were repeated with the second fictional trichome having a relatively thick, uniform wall thickness ($6\,\mu m$; Fig. 4a) with similar results (Fig. 4b,c,j,k). Although buckling occurred, it was in a location different from that observed experimentally (Fig. 1).

The thin and thick wall values specified earlier were taken from minimum and maximum thickness values that we and others measured (Kulich *et al*. 2015). However, as studied in detail by Kulich *et al*. (2015), and readily observed in our own images, the wall is far from uniform along its length. We thus assessed the possible importance of systematically graded wall thickness. We first examined the internal as well as external outlines of the trichome walls from plants grown precisely as for the earlier mentioned figures. We characterized them by using UV and DIC microscopies; both kinds of
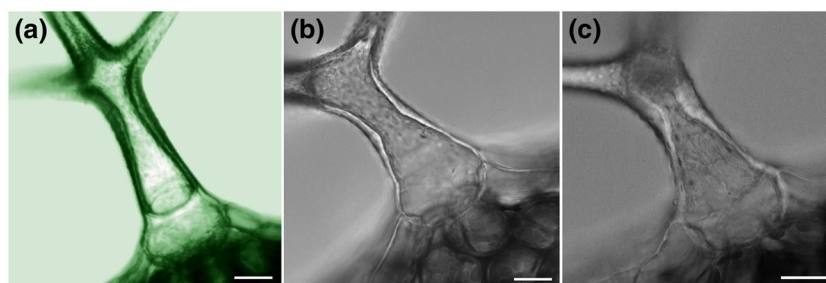

Figure 5. Non-uniform wall thickness. UV imaging (a) of the gross trichome structure permits the observation that the thickness of the wall is varied as in the model of Fig. 4d–f. Branch walls are thickened from tip to junction. Thickening is most prominent in the junction, the neck and the stalk basal to it. DIC imaging (b) confirms the thickening pattern. A detail in Fig. 5a not shown on the particular plane shown in Fig. 5b is an apparent discontinuity between pliant zone and podium. Comparison of Fig. 5a–c shows the variability in the neck region. Bars: $20\,\mu m$.

imaging (Fig. 5a,b,c) show thick walls in the branches, which increase in thickness as the branches join with the stalk and continue thick in the neck and the subjacent stalk. Where the thickened zone terminated, thickness tapered rapidly towards the pliant zone and remained thin in the podium. (The pliant zone is dark in the apo-pHusion images of Fig. 1.) Walls were thin in the skirt cells as well. We performed more subtle measurements on longitudinal sections visualized for other purposes with TEM. From the neck almost to the basal termination of the thickened zone, the average thickness was 6 μm, decreasing about 250 nm over that distance. Near the termination of the thickened zone, the thickness was about 1 μm.

Note incidentally that a distinct edge or border sometimes marks the place where the pliant zone and the surface portion of the podium meet. This border was conspicuous in some trichomes (see especially Fig. 5a) but was not readily visible in others. Staining axial sections with auramine O (for organic aldehydes) indicated that the ring, when present, was not always identically situated. A comparable gross geometry can be seen in a number of single-cell, uniseriate, and multicellular trichomes of other species. Although this structural feature might well make a contribution to force focusing, it was late to develop and thus did not seem universally essential for function. Thus, it was not taken into account in modelling. The structure was named the Ortmannian ring by Kulich *et al.* (2015), who described its development and variability in considerable detail.

Based on the measurements of gross taper described earlier and ignoring the very mild distributive taper and the seemingly mechanically unnecessary ring, a wall thickness that varied between 1.5 and 6 μm was assigned to a digital trichome (Fig. 4d). This simulated trichome responded to force application in much the same way as the real trichomes we imaged: after mild lateral loading, buckling occurred at the podium as in the experiments, with elevated strain energy density concentrated in this region (Fig. 4e). After mild axial compression, force focusing was also evident at the podium (red band indicating high strain energy density in Fig. 4f). The elevation of strain energy at the podium of this physiologically tapered trichome was substantially greater than elevations observed in the uniform-walled fictional trichomes.

In all simulations except that for the thick trichome plotted in Fig. 4k, the trichomes buckled at a critical load (peaks in plots of Fig. 4j,k). The reason the thick trichome did not buckle was that the applied force was not great enough. The stiffness (slope of curve) and critical loads of the trichomes were an order of magnitude lower for lateral loading than for axial loading, suggesting that lateral loading might be the dominant mode for sensing. The critical load for buckling in response to a lateral force was about 8 mN, a force that should be exerted by several kinds of insects feeding on Arabidopsis (Bidart-Bouzat & Kliebenstein 2011; Louis *et al.* 2012; Appel & Cocroft 2014).

Taken together, the results support the view that the properties of the Arabidopsis trichome wall have evolved to promote force focusing on and buckling instability within the pliant zone and podium. Thence, tension and compression can be experienced in the skirt with physiological consequences and are indeed transferred to the surrounding cells. From the biophysical point of view, the concept of functional force

transmission is well enough substantiated that it should be considered part of the body of knowledge about the trichome.

DISCUSSION

Contributing to our motivation to investigate mechanically elicited Ca^{2+} responses in Arabidopsis was the knowledge that cytosolic Ca^{2+} participates in elevations of secondary metabolism such as those that accompany several stresses (Ravilious & Jez 2012). Mechanosensitive production of toxic metabolites remains for consideration elsewhere, but we suspect that the result of the sensory activities we describe here is the greater production of chemical deterrents and their storage as well as facilitated release. More immediately and subtly, it might represent conditioning or 'priming' of the toxin-production system to enable a strong rapid response in the future, somewhat as described in the mechanosensory experiments described by Appel & Cocroft (2014).

While Ca^{2+} oscillations in the skirt cells are not a surprising result of mechanically stimulating the trichome, the alkaline shift of skirt and epidermal cell apoplasts was unexpected. Could it trigger or represent a shift in metabolism favouring the production of defence compounds? Or, possibly, could it be associated more directly with a change in wall properties?

If the Arabidopsis trichome is indeed a sensory switch for detecting touch by potential attacking insects, it must follow that some potential herbivores are of a size that can disturb trichomes. The 8 mN buckling load of the trichomes is several times the weight of some weevil beetles and their mature caterpillars. Assuming that forces exerted on individual trichomes by such insects are on the order of a few times their body weight, this value suggests that force focusing culminating in buckling plays a role in trichome-based mechanosensing that might help limit insect numbers. Extending the argument, on one the hand, some of the most successful herbivores, such as aphids, appear to be of weights too small to disturb the trichome substantially. On the other hand, herbivory by relatively larger insects such as feeding cabbage loopers, beet army worms or *Pieris rapae* caterpillars might effectively perturb the trichomes.

We hypothesize that mechanical disturbance by ovipositing adults might be more significant for priming than stimulation by caterpillars directly applied as by Appel & Cocroft (2014). Some kinds of moths and butterflies, such as those of *Pieris* (Terofal 1965; Chew & Renwick 1995; Bauer *et al.* 1998), 'drum' leaves with their tarsi and drag their antennae over leaves to test their suitability for ovipositing. Drumming and dragging, demonstrated not to wound the leaf surface, are known to serve the butterfly as a mechanism for sampling surface chemicals such as glucosinolates (Chew & Renwick 1995). While the secondary metabolites evidently evolved to discourage ravaging by caterpillars, the butterflies depend on them as attractants, and at least some caterpillars that feed on them (Chun 1972) thrive and repulse predatory birds. In turn, however, Arabidopsis might utilize the butterflies in much the way described for experimentally applied *Pieris* caterpillars by Appel & Cocroft (2014). That is, the plant as well as the butterfly might utilize drumming for information. It makes sense

that priming should have evolved so that leaves would not overreact to egg deposition but would be ready to escalate costly secondary metabolism immediately when larvae emerge. Given the importance of priming, it appears that the plant may have developed paired chemical and physical receptor systems to notify it about egg deposition.

As a final note to the evaluation of whether and how insects might perturb the trichome mechanically, we emphasize that the virtual parameters for variable wall thickness and the isotropic material properties used were only close approximations, and (reflecting the subtlety of the wall morphology) they can be optimized to produce critical loads less than 8 mN. Moreover, it is important in extending our studies to other plants that taper proportions of the wall rather than the absolute values of wall thickness can determine how force is transmitted and focused.

Arabidopsis is capable of many regulatory decisions about the activation of specific branching pathways of toxin synthesis in response to environmental conditions (Wittstock & Burow 2010; Frerigmann & Gigolashvili 2014). We propose that force sensing by its trichomes helps not only simply to enhance toxin production but also to enhance the regulatory flexibility of production. It will be particularly interesting to learn if general Ca^{2+} elevation and skirt cell Ca^{2+} oscillation might serve to steer secondary metabolism along different pathways and hence yield different balances of toxin output. In any case, mechanosensing likely serves a special role in helping ward off some herbivores by initiating responses before extensive damage can be done.

Mechanoresponses of plant cells are often mediated by mechanosensitive Ca^{2+}-selective ion channels (Telewski 2006; Monshausen & Gilroy 2009; Hamilton *et al.* 2015). It is interesting that one class of such channels is modulated by lowering of temperature (Ding & Pickard 1993a,1993b) – at least rapid lowering – as well as to cell membrane deformation by applied force. Perhaps the regulation of secondary metabolites by temperature sensing and mechanosensing are related at the membrane level in the Arabidopsis trichome system, although there are other sensory possibilities for both modalities. It would further be interesting to check whether voltage and pH modulation of such channels (Ding & Pickard 1993a,1993b; Ding *et al.* 1993) might participate in detection of the microbial invasion of Arabidopsis leaves or in related feedbacks involving transmembrane ion movement.

Arabidopsis belongs to the *Brassica* or mustard family, which is represented by many crop plants. Some of these might also have mechanically regulated active trichome systems. Moreover, plants in certain other families bear trichomes with a basal architecture remindful of that in Arabidopsis. Some of these trichomes might be mechanosensory, despite, in at least most cases, producing entirely different secondary metabolites. Could the activity of trichomes such as these be agriculturally enhanced by leaf-stroking procedures – or even acoustic vibration – to increase herbivore resistance on a controlled basis? Moreover, although in the experiments of Appel & Cocroft (2014) wind did not elicit the kinds of toxin metabolism that *Pieris* feeding does, bending leaves per se might promote different defence responses in Arabidopsis and in many species,

because even non-specialist cells can increase Ca^{2+} levels and alter hormone levels in response to mechanical stimulation (Telewski 2006; Knight *et al.* 1992; Abeles *et al.* 1992).

Additional support for our hypothesis comes from the study of mutants, although we emphasize that too little is known about the trichome wall structure and the complexity of its multiple functions, which may include final steps in the production of toxins (Dai *et al.* 2010; Wittstock & Burow 2010; Frerigmann *et al.* 2012; Kulich *et al.* 2015) to read too much into this. Most applicable is a test provided by a mutant recently described by Kulich *et al.* (2015) (the EXO70H4-1 mutant) that does not create a secondary trichome wall, without which there is no taper in the trichome stalk. Compression causes it to bend in flexure (Kulich *et al.* 2015) much like the fictional finite-element model with a thin uniform wall. The basis of this mutant architecture is the lack of secondary wall callose, a glycopolymer predominant in a number of specialized secondary walls. Apparently, callose production and trichome maturation as a whole are interactively linked. However, callose is not the only mechanically relevant constituent to be found in the secondary wall, and so the combination of diminished wall strength and wall taper confounds interpretation. Our model does not address the strength per unit volume or the length of the wall (a material property of the trichome) but rather the value of taper (a structural property of the trichome). If a mutant could be found in which the only special feature was extension of secondary wall into the buckling region, a definitive test of the central prediction of the model could be performed.

Finally, are there homologous or analogous trichomes or appendages described in the literature? Peiffer *et al.* (2009) (see commentary in Tooker *et al.* (2010)) classify the breaking of glandular heads of one class of tomato trichomes as mechanoresponses. The release of materials from burst glands and from true wounding both contribute to defence responses by direct release of chemicals stored within the wounded cell and by initiating signalling cascades within the cell. However, this is distinct from the Ca^{2+} signalling, pH response and non-damaging buckling explored in the current study. While there is a large literature on the leaves and trigger trichomes of the carnivores *Dionaea* and *Aldrovanda* (cf. Williams 2002), these complex multicellular elastic structures utilize a rocker mechanism to initiate receptor potentials and in turn action potentials, leading in *Dionaea* to apoplastic acidification of a critical zone of cells. We believe that ours is the first study to quantify responses of trichomes (in non-carnivorous plants) that can elastically signal surrounding cells to undertake Ca^{2+} oscillations and apoplastic alkalization.

In sum, the gross structure of the Arabidopsis trichome system appears to be a buckling-activated switch that initiates a mediational signalling activity in response to touching, bending or rubbing. The trichome appears tailored to elicit this function through its unique tapering and through harnessing of a buckling instability at high loads and force focusing at lower loads. The biophysical evidence we present suggests a well-adapted mechanical system consisting of tapered wall, pliant zone, podium and skirt cells that endow the trichome with the capacity for functional force transmission.

Our findings for mechanosensing by Arabidopsis trichomes may have implications for those of other plants whether considered active secretors or considered passive. Exploration of such possibilities might significantly extend understanding of the relationships between plants and the insects that interact with them.

Conflict of interests

The authors declare that they have no conflicts of interest.

AUTHORS' CONTRIBUTIONS

L.H.Z., G.M.G and B.G.P. conceived and initiated the project. L.H.Z. and B.G.P. designed and performed the experiments. G.M.G., T.J.L., F.X., L.H.Z. and B.G.P. designed the numerical analyses. S.B.L. and P.F.W. performed the simulations and analysis. L.H.Z., B.G.P. and G.M.G. composed the manuscript. All authors analysed the results and edited the manuscript.

REFERENCES

Abeles F.B., Morgan P.W. & Saltveit M.E. Jr. (1992) *Ethylene in Plant Biology* 2nd edn. Academic Press, San Diego.

Allen G.J., Kwak J.M., Chu S.P., Llopis J.L., Tisen R.Y., Harper J.F. & Schroeder J.I. (1999) Cameleon calcium indicator reports cytoplasmic calcium dynamics in Arabidopsis guard cells. *Plant Journal* **19**, 735–747.

Appel H.M. & Cocroft R.B. (2014) Plants respond to leaf vibrations caused by insect herbivore chewing. *Oecologia* **175**, 1257–1266.

Bauer R., Haribal M., Renwick J.A.A. & Stadler E. (1998) Contact chemoreception related to host selection and oviposition behavior in the monarch butterfly, *Danaus plexippus*. *Physiological Entomology* **23**, 7–19.

Bidart-Bouzat M.G. & Kliebenstein D. (2011) An ecological genomic approach challenging the paradigm of differential plant responses to specialist versus generalist insect herbivores. *Oecologia* **167**, 677–689.

Chew F.S. & Renwick J.A.A. (1995) Host plant choice in *Pieris* butterflies. In *Chemical Ecology of Insects Vol. 2* (eds Cardé R.T. & Bell W.), pp. 214–238. Chapman & Hall, New York.

Chun M.W. (1972) *Dynamics of Feeding Responses in Pieris brassicae* Linn as a Function of Chemosensory Input: a Behavioural, Ultrastructural and Electrophysiological Study. H. Veenman, Wageningen.

Clapham D.E. (2007) Calcium signaling. *Cell* **131**, 1047–1058.

Dai X., Wang G., Yang D.S., Tang Y., Broun P., Marks D.M., … Zhao P.X. (2010) TrichOME: a comparative omics database for plant trichomes. *Plant Physiology* **152**, 44–54.

Ding J.P., Badot P.M. & Pickard B.G. (1993) Aluminium and hydrogen ions inhibit a mechanosensory calcium-selective cation channel. *Australian Journal of Plant Physiology* **20**, 771–778.

Ding J.P. & Pickard B.G. (1993a) Mechanosensory calcium-selective cation channels in epidermal cells. *Plant Journal* **3**, 83–110.

Ding J.P. & Pickard B.G. (1993b) Modulation of mechanosensitive calcium-selective cation channels by temperature. *Plant Journal* **3**, 713–720.

Frerigmann H., Böttcher C., Baatout D. & Gigolashvili T. (2012) Glucosinolates are produced in trichomes of *Arabidopsis thaliana*. *Frontiers in Plant Science.* **3**, 242. DOI:10.3389/fpls2012.00242.

Frerigmann H. & Gigolashvili T. (2014) MYB34, MYB51, and MYB122 distinctly regulate indolic glucosinolate biosynthesis in *Arabidopsis thaliana*. *Molecular Plant* **7**, 814–828.

Gjetting K.S.K., Ytting C.K., Schulz A. & Fuglsang A.T. (2012) Live imaging of intra- and extracellular pH in plants using pHusion, a novel genetically encoded biosensor. *Journal of Experimental Botany* **63**, 3207–3218.

Hamilton E.S., Schlegel A.M. & Haswell E.S. (2015) United in diversity: mechanosensitive ion channels in plants. *Annual Reviews of Plant Biology* **66**, 113–137.

Hepler P.K. & Gunning B.E. (1998) Confocal fluorescence microscopy of plant cells. *Protoplasma* **201**, 121–157.

Holdaway-Clarke T.L., Walker N.A., Hepler P.K. & Overall R.L. (2000) Physiological elevations in cytoplasmic free calcium by cold or ion injection result in transient closure of higher plant plasmodesmata. *Planta* **2**, 329–335.

Knight M.R., Smith S.M. & Trewavas A.J. (1992) Wind-induced plant motion immediately increases cytosolic calcium. *Proceedings of the National Academy of Science USA* **89**, 4967–4971.

Kulich I., Vojtíková Z., Glanc M., Ortmannová I.J., Rasmann S. & Žárský V. (2015) Cell wall maturation of Arabidopsis trichomes is dependent on exocyst subunit13 EXO70H4 and involves callose deposition. *Plant Physiology Preview. March* **12**, 2015. DOI:10.1104/pp.15.001.

Link K., Vogel F. & Sonnewald U. (2011) PD trafficking of potato leaf roll virus movement protein in Arabidopsis depends on site-specific protein phosphorylation. *Frontiers in Plant Science* **2**, 1–10.

Louis J., Singh V. & Shah J. (2012) *Arabidopsis thaliana*–aphid interaction. *Arabidopsis Book/ American Society of Plant Biologists* **10**, e0159.

Monshausen G.B., Messerli M.A. & Gilroy S. (2008) Imaging of the yellow cameleon 3.6 indicator reveals that elevations in cytosolic Ca^{2+} follow oscillating increases in growth in root hairs of Arabidopsis. *Plant Physiology* **147**, 1690–1698.

Monshausen G.B. & Gilroy S. (2009) Feeling green: mechanosensing in plants. *Trends in Cell Biology* **19**, 228–235.

Monshausen G.B. & Haswell E.S. (2013) A force of nature: molecular mechanisms of mechanoperception in plants. *Journal of Experimental Botany* **64**, 4663–4680.

Paul-Victor C., Züst T., Rees M., Kliebenstein D.J. & Turnbull L.A. (2010) Mew method for measuring relative growth rate can uncover the costs of defensive compounds in *Arabidopsis thaliana*. *New Phytologist* **187**, 1102–1111.

Peiffer M., Tooker J.F., Luthe D.S. & Felton G.W. (2009) Plants on early alert: glandular trichomes as sensors for insect herbivores. *New Phytologist* **184**, 644–656.

Ravilious G.E. & Jez J.M. (2012) Structural biology of plant sulfur metabolism: from assimilation to biosynthesis. *Natural Products Reports* **29**, 1138–1152.

Schindelin J., Arganda-Carreras I., Frise E., Kaynig V., Longair M., Pietzsch T., … Cardona A. (2012) Fiji: an open-source platform for biological-image analysis. *Nature Methods* **9**, 676–682.

Suo B., Seifert S., Kirik V. & Table S. (2013) Arabidopsis GLASSY HAIR genes promote trichome papillae development. *Journal of Experimental Botany* **64**, 4981–4991.

Swanson S. & Gilroy S. (2013) Imaging changes in cytoplasmic calcium using the yellow cameleon 3.6 biosensor and confocal microscopy. *Methods in Molecular Biology* **1009**, 291–302.

Tanaka K., Swanson S.J., Gilroy S. & Stacey G. (2010) Extracellular nucleotides elicit cytosolic free calcium oscillations in Arabidopsis. *Plant Physiology* **154**, 705–719.

Telewski F.W. (2006) A unified hypothesis of mechanoperception in plants. *American Journal of Botany* **93**, 1466–1476.

Terofal F. (1965) On the problem of host specificity in Pieridae (Lepidoptera). With special consideration of the indigenous species *Pieris brassicae* L., *P. napi* L., and *P. rapae* L. *Mitteilungen der Münchner Entomologischen Gesellschaft* **55**, 1–76.

Tooker J.F., Peiffer M., Luthe D.S. & Felton G.W. (2010) Trichomes as sensors: detecting activity on the leaf surface. *Plant Signaling and Behavior* **5**, 73–75.

Williams S.E. (2002) Comparative physiology of the *Droseraceae sensu stricto* – How do tentacles bend and traps close? *Proceedings of the 4th International Carnivorous Plant Conference*, *Tokyo*, *Japan*. 77-81.

Wittstock U. & Burow M. (2010) Glucosinolate breakdown in Arabidopsis: mechanism, regulation and biological significance. *Arabidopsis Book / American Society of Plant Biologists* **8**, e0134.

Züst T., Joseph B., Shimizu K.K., Kliebenstein D.J. & Turnbull L.A. (2011) Using knockout mutants to reveal the growth costs of defensive traits. *Proceedings of the Royal Society of London B: Biological Sciences* **278**, 2598–2603.

SUPPORTING INFORMATION

Additional Supporting Information may be found in the online version of this article at the publisher's web-site:

Figure S1. Two views of a representative finite-element mesh.

Figure S2. The nipple of a baby bottle provides a mechanical analogue for trichome structure and buckling. The widening of the nipple towards the base of the cap promotes buckling instabilities analogous to those observed in the trichome. The application of a central mechanical load encourages a force-focusing buckling instability at the base, as in Figs. 1 and 4e. Application of a mechanical load that is slightly off axis encourages such buckling at a lower level of applied force, as in Figs. 3b and 4f. Evidence suggests that the long branches of the trichome cells and the spatial grading of the trichome cell wall thickness further promote such force-focusing instability.

Figure S3. Graphical representation of oscillations evidenced in Supporting Information Movie 2, with statistics. ROI numbers correspond to those in Fig. 2b. Student's *t*-tests indicated that when comparing ROI 10 with ROI 1 (and with ROIs 2–9), Ca^{2+} oscillations were distinguishable statistically with *P* values < 0.00001.

Figure S4. Graphical representation of oscillations evidenced in Supporting Information Movie S3, with statistics. ROI numbers correspond to those in Fig. 2c. Student *t*-tests indicated that when comparing ROI 10 with ROI 1 (and with ROIs 2–9), Ca^{2+} oscillations were distinguishable statistically with *P* values < 0.00001.

Movie S1. In a movie kindly provided by David W. Ehrhardt, fluorescence-labelled plasmodesmata are seen connecting the skirt cells of the trichome with each other as well as with the neighbouring cells that are captured in the image. However, they are not seen in the podium or stalk of the trichome.

Movie S2. The image stack from which Fig. 1c was projected. With a strong lateral push, the trichome buckles so severely that the stalk is laid almost parallel to the epidermal surface. (The stack does not capture the complete trichome.)

Movie S3. Imaged cameleon shifts in the skirt cells of Fig. 2b.

Movie S4. Imaged cameleon shifts in the skirt cells of Fig. 2c.